

Facile Si–H bond activation and hydrosilylation catalysis mediated by a nickel–borane complex†

Cite this: *Chem. Sci.*, 2014, 5, 590Samantha N. MacMillan,^a W. Hill Harman^b and Jonas C. Peters^{*a}

Metal–borane complexes are emerging as promising systems for study in the context of bifunctional catalysis. Herein we describe diphosphineborane nickel complexes that activate Si–H bonds and catalyze the hydrosilylation of aldehydes. Treatment of $[\text{Mes}^{\text{D}}\text{DPB}^{\text{Ph}}]\text{Ni}$ (**1**) ($[\text{Mes}^{\text{D}}\text{DPB}^{\text{Ph}}] = \text{MesB}(\text{o-Ph}_2\text{PC}_6\text{H}_4)_2$) with organosilanes affords the complexes $[\text{Mes}^{\text{D}}\text{DPB}^{\text{Ph}}](\mu\text{-H})\text{NiE}$ ($\text{E} = \text{SiH}_2\text{Ph}$ (**3**), SiHPh_2 (**4**)). Complex **4** is in solution equilibrium with **1** and the thermodynamic and kinetic parameters of their exchange have been characterized by NMR spectroscopy. Complex **1** is a catalyst for the hydrosilylation of a range of *para*-substituted benzaldehydes. Mechanistic studies on this reaction *via* multinuclear NMR spectroscopy are consistent with the intermediacy of a borohydrido-Ni-siloxyalkyl species.

Received 18th September 2013

Accepted 22nd October 2013

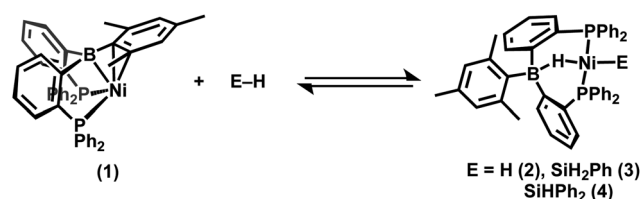
DOI: 10.1039/c3sc52626g

www.rsc.org/chemicalscience

Introduction

The metal-mediated activation of Si–H bonds provides a direct and efficient strategy for the functionalization of organic substrates.¹ In these hydrosilylation processes, the oxidative addition of an Si–H bond to the metal center is invoked as one of the first steps of the catalytic cycle.² While Si–H oxidative additions are known for metals of the nickel triad,^{1b,3,4,5} H–Ni–SiR₃ species are less well-studied in comparison to their Pt counterparts, presumably due to their instability and high degree of reactivity.^{1b} The use of bulky or chelating ligands has allowed for the isolation of a number of mononuclear Ni silyl (Ni–SiR₃)^{3a,6} and Ni silane^{6a,7} complexes. However, well-characterized mononuclear H–Ni–SiR₃ complexes, which would be expected from the oxidative addition of an Si–H bond at Ni, are rare.^{7b,8}

We recently reported the preparation of a nickel–borane complex, $[\text{Mes}^{\text{D}}\text{DPB}^{\text{Ph}}]\text{Ni}$ (**1**), that reversibly activates H₂ to generate the borohydrido-hydride species $[\text{Mes}^{\text{D}}\text{DPB}^{\text{Ph}}](\mu\text{-H})\text{Ni}(\text{H})$ (**2**, Scheme 1), and catalyzes olefin hydrogenation.⁹ Intrigued by this bifunctional reactivity and its promise for realizing 2-electron catalytic processes using late first-row transition metals, we sought to broaden our knowledge of the reaction chemistry of **1**. We reasoned that analogous H–Ni–SiR₃ species might be accessible as a consequence of the stabilizing interaction of the boron center. Herein we report the preparation of well-characterized borohydrido-Ni-silyl



Scheme 1

complexes derived from the oxidative addition of Si–H substrates to a Ni–B core and probe the mechanism of benzaldehyde hydrosilylation by **1**.

Results and discussion

Preparation and solid-state molecular structures of borohydrido-Ni-silyl complexes

Treatment of **1** at room temperature with one equivalent of phenylsilane or diphenylsilane results in immediate Si–H bond cleavage to afford the borohydrido-silyl complexes $[\text{Mes}^{\text{D}}\text{DPB}^{\text{Ph}}](\mu\text{-H})\text{NiSiH}_2\text{Ph}$ (**3**) and $[\text{Mes}^{\text{D}}\text{DPB}^{\text{Ph}}](\mu\text{-H})\text{NiSiHPh}_2$ (**4**), respectively (Scheme 1). Yellow-orange **3** and orange **4** are diamagnetic, air-sensitive solids and are reliably isolated in *ca.* 75% yield. Although analytically pure samples of **4** can be isolated in the solid state by crystallization, upon dissolution an equilibrium mixture of **4**, **1** and free H_2SiPh_2 results (*vide infra*).

The ¹H NMR spectra of **3** and **4** each feature two signature resonances, one corresponding to the Si–H protons and one broad, upfield shifted resonance corresponding to the bridging hydride. The Si–H resonance of **3** is a sharp triplet centered at 4.30 ppm (³J_{HIP} = 9.2 Hz, ¹J_{HSi} = 138 Hz), while the bridging borohydride resonance appears at –2.47 ppm; as expected, these peaks integrate in a 2 : 1 ratio (Fig. 1). Similarly, the ¹H NMR spectrum of **4** displays two resonances that integrate in a

^aDivision of Chemistry and Chemical Engineering, California Institute of Technology, Pasadena, CA 91125, USA. E-mail: jcpeters@caltech.edu; Tel: +1 626 395 4036

^bDepartment of Chemistry, University of California, Riverside, CA 92521, USA

† Electronic supplementary information (ESI) available: Experimental procedures and crystallographic data. CCDC 961588, 961589 and 961590. For ESI and crystallographic data in CIF or other electronic format see DOI: 10.1039/c3sc52626g

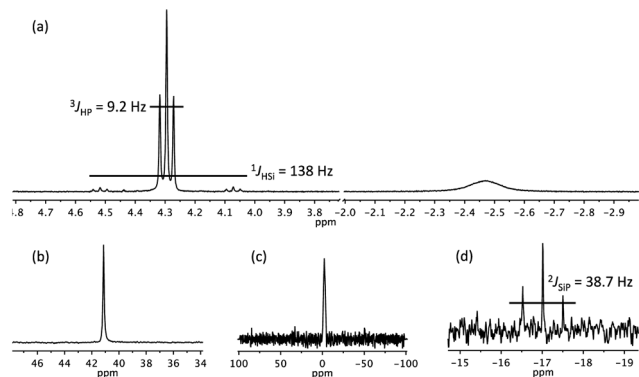


Fig. 1 Signature resonances in the (a) ^1H , (b) $^{31}\text{P}\{^1\text{H}\}$, (c) $^{11}\text{B}\{^1\text{H}\}$ and (d) $^{29}\text{Si}\{^1\text{H}\}$ NMR spectra for **3**.

1 : 1 ratio (5.01 ppm, t, Si-H, $^3J_{\text{HP}} = 14.7$ Hz, $^1J_{\text{HSi}} = 88$ Hz and -2.61 ppm, s, B-H-Ni). The $^{31}\text{P}\{^1\text{H}\}$ NMR spectra each display a singlet at ca. 40 ppm, similar to the borohydrido-hydride complex **2**; no $^2J_{\text{HP}}$ was resolved at room temperature for **3** or **4**. The $^{11}\text{B}\{^1\text{H}\}$ NMR resonances of -2.2 ppm for complex **3** and -1.7 ppm for complex **4** are sharpened and shifted upfield relative to **1** (21.6 ppm), indicative of increased electron density at boron. The $^{29}\text{Si}\{^1\text{H}\}$ NMR spectra each display a triplet centered at -17.0 ppm ($^2J_{\text{SiP}} = 38.7$ Hz) and 3.1 ppm ($^2J_{\text{SiP}} = 37.9$ Hz) for **3** and **4**, respectively. The upfield shift of the $^{29}\text{Si}\{^1\text{H}\}$ NMR resonance for the secondary versus primary silyl species is consistent with that observed in the literature.^{5b} The Si-H stretches in the IR spectra for **3** and **4** are observed at 2060 and 2058 cm^{-1} , respectively.

The previously reported equilibrium between **1** and the borohydrido-hydride complex **2** could be studied in solution. However, removal of the H_2 atmosphere resulted in rapid H_2 loss from **2** to regenerate **1**, and the equilibrium process frustrated the growth of single crystals of **2** and the acquisition of X-ray structural data. Gratifyingly, the molecular structures of **3** and **4** could be determined by single-crystal X-ray diffraction and support our previous structural assignment of **2**. The solid-state structure of **4** features two independent molecules in the

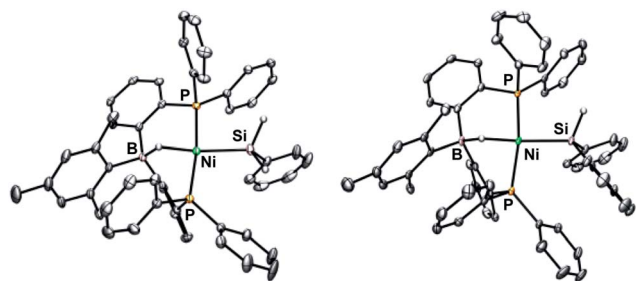


Fig. 2 Solid-state structures of **3** (left) and **4** (right). Thermal ellipsoids are drawn at 50% probability. Hydrogen atoms bound to carbon and a molecule of ether (**3**) and benzene (**4**) are omitted for clarity. Selected bond lengths (\AA) and angles ($^\circ$) for **3**: Ni-Si 2.2379(4); Ni-H 1.58(2); Ni-B 2.440(2); B-H 1.31(2); H-Ni-Si 168.3(6); **4** (avg): Ni-Si 2.2479(7); Ni-H 1.64(3); Ni-B 2.506(3); B-H 1.27(3); H-Ni-Si 163.36(9).

asymmetric unit, one of which is shown in Fig. 2. Both **3** and **4** feature a distorted square planar geometry at nickel with two *trans*-disposed phosphine donors, a terminal silyl group, and a hydride bridging the nickel and boron centers (Fig. 2). The nickel centers of **3** and **4** lie slightly outside the P-Si-P plane (**3**: 0.036 \AA ; **4**: 0.047 and 0.085 \AA). The Ni-Si distance of $2.2379(7)$ \AA for **3** and $2.2435(7)$ \AA (avg) for **4** is in the range of other monomeric nickel complexes containing a monodentate silyl fragment (2.19 – 2.37 \AA),^{6a-c,7b,8,10} for example $2.239(8)$ \AA in the unusual hydrido-silyl complex $[\text{Ni}(\text{AlCp}^*)_3(\text{H})(\text{SiEt}_3)]$ reported by Fischer.^{10c}

Solution studies of $[\text{Mes}^*\text{DPB}^{\text{Ph}}](\text{H})\text{NiSiHPh}_2$ (**4**)

The well-defined solution equilibrium of **1** and **4** (Scheme 1) provided the opportunity to study both the thermodynamics and kinetics of Si-H bond activation by **1**. Dissolution of pure **4** in C_6D_6 gives an equilibrium mixture of **1**, **4** and H_2SiPh_2 , corresponding to a $K_{\text{eq}} \approx 960$ M^{-1} . A van't Hoff analysis over a 50 K range yielded thermal parameters of $\Delta H = -12 \pm 1$ kcal mol^{-1} and $\Delta S = -27 \pm 3$ eu. Repeating the experiment with D_2SiPh_2 yielded thermal parameters of $\Delta H = -20 \pm 1$ kcal mol^{-1} and $\Delta S = -47 \pm 3$ eu, with an inverse equilibrium isotope effect of $\text{EIE}_{328} = 0.18$.¹¹

The kinetics of the Si-H bond activation process defined in Scheme 1 were studied by two-dimensional exchange spectroscopy (2D EXSY).¹² ^1H - ^1H EXSY spectra were recorded in toluene- d_8 over a 40 K range with mixing times (T_m) of 0 ms and 700 ms. A representative spectrum is shown in Fig. 3. The forward (k_1) and reverse (k_{-1}) rate constants were extracted from the EXSY data and the results are shown in Table 1. Eyring analysis of these data gave $\Delta H^\ddagger = 3.9 \pm 1$ kcal mol^{-1} and $\Delta S^\ddagger = -39 \pm 3$ eu for the forward reaction and $\Delta H^\ddagger = 17 \pm 1$ kcal mol^{-1} and $\Delta S^\ddagger = -9.6 \pm 3$ eu for the reverse process. The analogous reaction of **1** with D_2SiPh_2 proved too slow to be studied by EXSY.

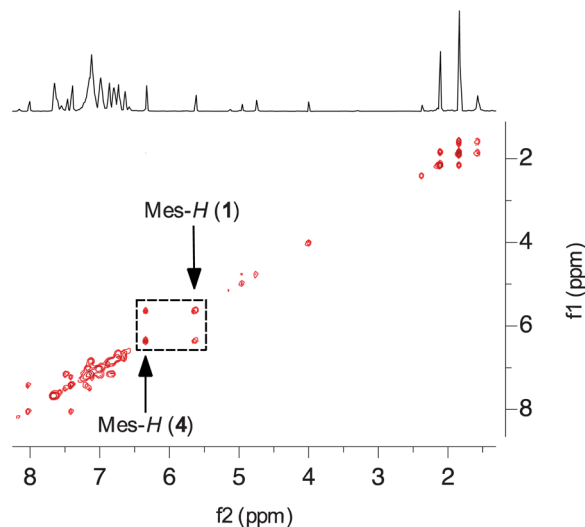


Fig. 3 Representative 2D ^1H - ^1H EXSY spectrum of **4** taken at 348 K with $T_m = 700$ ms in toluene- d_8 .

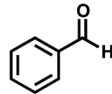
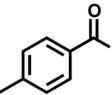
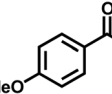
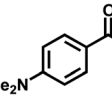
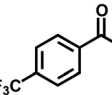
Table 1 Summary of rate data extracted from 2D $^1\text{H}-^1\text{H}$ EXSY spectra of **4**

T (K)	327	337	347	357
k_1 ($\text{M}^{-1} \text{s}^{-1}$)	43	51	67	73
k_{-1} (s^{-1})	0.16	0.36	0.79	1.4
k_1/k_{-1} (M^{-1})	270	140	85	50

Catalytic hydrosilylation reactivity

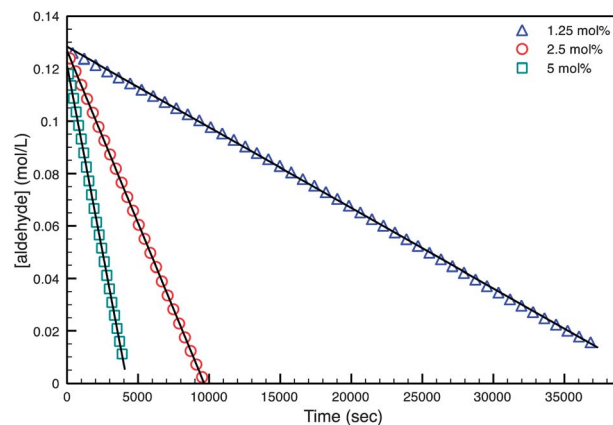
In an effort to incorporate this Si-H bond activation process into a useful catalytic cycle, we examined the hydrosilylation of *para*-substituted benzaldehydes. Catalytic hydrosilylation of benzaldehyde with 5 mol% **1** proved facile and was accomplished in 99% yield within 6 h at room temperature (Table 2, entry 1). Catalyst **1** tolerated the electron-donating and electron-withdrawing groups shown in Table 2. In contrast to the iron pyridinediimine system recently reported by Chirik,¹³ the rate of hydrosilylation by **1** increased as a function of placement of more electron-donating substituents at the *para* position (entry 4). The hydrosilylation transformation was found to be zero order in both benzaldehyde and H_2SiPh_2 and first order in catalyst (Fig. 4). The reaction solution remained transparent throughout the catalysis and mercury had no effect on the catalytic rate or the products of the reaction, consistent with a homogeneous catalytic system.

Table 2 Summary of results of catalytic hydrosilylation of *para*-substituted benzaldehydes by **1**

Entry ^a	Substrate	Conversion; time	Chemical yield ^b
1		>98%; 5.9 h	99%
2		>98%; 2.5 h	97%
3		>98%; 2.7 h	98%
4		>98%; 44 min	98%
5		>98%; 4.6 days	92%

^a 1 mmol substrate, 1 mmol H_2SiPh_2 , 5 mol% **1**, 500 μL C_6D_6 .

^b Determined by NMR integration against an internal standard.

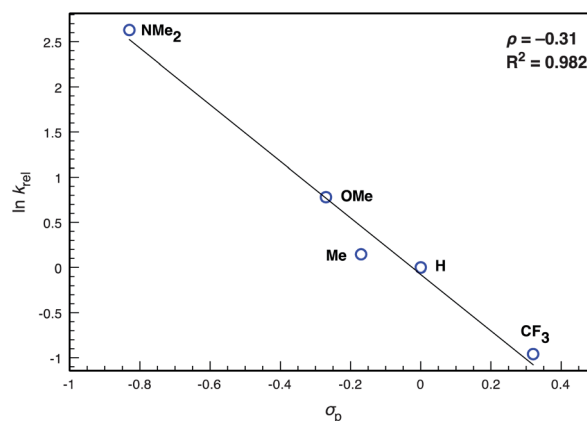
**Fig. 4** Plot of aldehyde concentration versus time for the hydrosilylation of *p*-dimethylaminobenzaldehyde by 1.25, 2.5, and 5 mol% **1**.

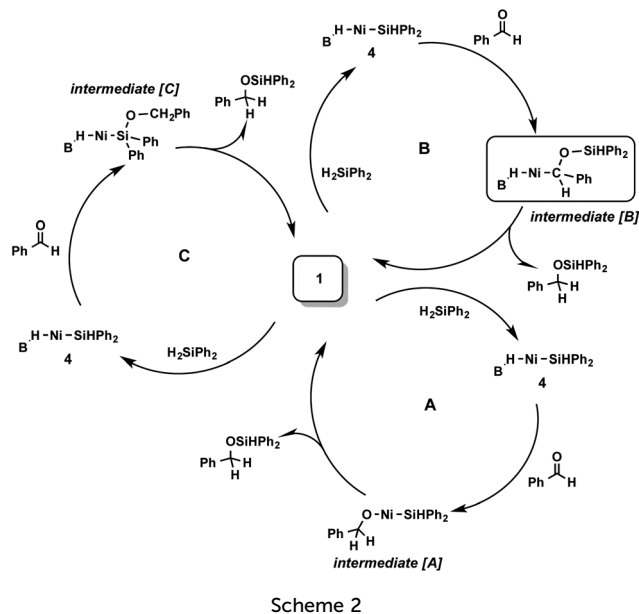
Competition experiments were carried out to explore substituent effects on the rate of hydrosilylation. For each experiment, the hydrosilylation of two equimolar substrates was monitored (1 eq. benzaldehyde A: 1 eq. benzaldehyde B: 1 eq. H_2SiPh_2) using 5 mol% of **1**. The Hammett correlation of the relative rates of hydrosilylation is illustrated in Fig. 5 and shows that electron-donating substituents in the *para* position accelerate the rate of hydrosilylation.

Catalytic hydrosilylation mechanistic studies

Typically, the transition metal-catalyzed reduction of carbonyl functionalities is mediated by Rh, Pt and other precious metals.¹⁴ In recent years, however, there have been numerous efforts to incorporate more environmentally benign and less expensive first row metals, such as Ti,¹⁵ Fe,¹⁶ Ni,¹⁷ and Cu.¹⁸ Mechanistic proposals for these metal catalysts generally invoke a hydride mechanism in which a metal hydride species is generated, followed by carbonyl insertion into the M-H bond to give an alkoxide complex.

Three plausible mechanisms we have considered for the hydrosilylation of benzaldehydes catalyzed by **1** are outlined in

**Fig. 5** Hammett correlation diagram for the relative rates of hydrosilylation of *para*-substituted benzaldehydes by **1** and H_2SiPh_2 .



Scheme 2 (cycles A, B, and C). In each mechanism shown, H_2SiPh_2 adds to **1** to generate **4**. From here, benzaldehyde can insert into the Ni–H bond as described above, generating a Ni-alkoxide intermediate [A] depicted in cycle A, which can then undergo reductive elimination of the organic product to regenerate **1**. Alternatively, in an Ojima-type mechanism,¹⁹ benzaldehyde can insert into the Ni–Si bond to generate a borohydrido-siloxyalkyl intermediate [B] depicted in cycle B, followed by reductive elimination of the hydrosilylated product. Finally, in a Zheng–Chan-type mechanism,²⁰ benzaldehyde can insert into the Si–H bond to generate the intermediate species [C] shown in cycle C, which can then lose the organic product *via* reductive elimination to close the catalytic cycle.

To better understand the hydrosilylation process, stoichiometric reactions were carried out using $[\alpha\text{-}^{13}\text{C}]$ -benzaldehyde. Treatment of a toluene- d_8 solution of **1** with a stoichiometric amount of $[\alpha\text{-}^{13}\text{C}]$ -benzaldehyde yields a red solution with a singlet in the $^{31}\text{P}\{^1\text{H}\}$ NMR spectrum at 38.6 ppm. Upon cooling to -60°C , a ^1H NMR resonance at 5.99 ppm is present that is coupled to a $^{13}\text{C}\{^1\text{H}\}$ NMR resonance at 91.3 ppm (HSQC). In the proton-coupled ^{13}C NMR spectrum, the peak at 91.3 ppm splits into a doublet with $J_{\text{CH}} = 174$ Hz (free aldehyde: 190.9 ppm, d, $J_{\text{CH}} = 174$ Hz). The upfield shifts of the ^1H and ^{13}C resonances are indicative of substantial $\text{d} \rightarrow \pi^*$ back donation,²¹ consistent with other $\text{Ni}(\eta^2\text{-aldehyde})$ species reported in the literature.²²

Single crystals obtained from this reaction mixture were analyzed by X-ray diffraction to reveal $[\text{MesDPB}^{\text{Ph}}]\text{Ni}(\eta^2\text{-benzaldehyde})$ (**5**, Fig. 6). The nickel atom is formally three-coordinate with the benzaldehyde bound in an η^2 fashion. The $\text{C}=\text{O}$ linkage lies in the trigonal coordination plane; the sum of the angles around the benzaldehyde carbon is 354° and the phenyl ring is essentially coplanar to the $\text{C}=\text{O}$ bond. The $\text{C}-\text{O}$ bond length of 1.312(2) Å is slightly shorter than those reported for related $\text{Ni}(\eta^2\text{-carbonyl})$ complexes (1.32–1.34 Å),^{22b,23} for example, 1.345(2) Å in $[\text{Ni}(\eta^2\text{-HPhCO})(\text{dippe})]$ (dippe = 1,2-bis(diisopropylphosphino)ethane), reported by Cámpora.^{22a}

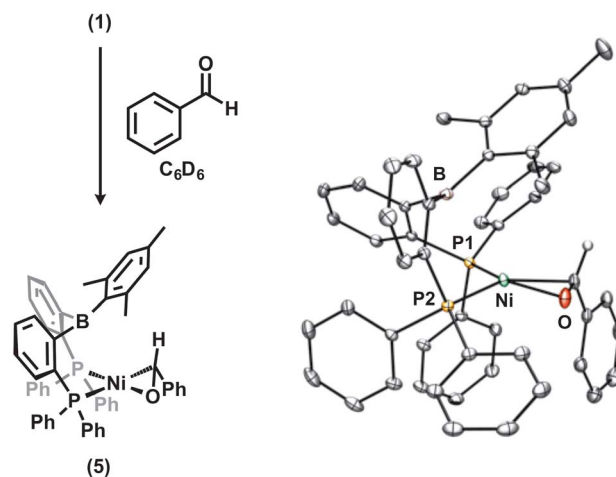


Fig. 6 Synthesis of **5** (left) and solid-state structure of **5** (right). Thermal ellipsoids are drawn at 50% probability. Solvent molecules and hydrogen atoms (except for that of the benzaldehyde carbon) are omitted for clarity. Selected bond lengths (Å) and angles ($^\circ$) for **5**: Ni–O 1.876(2); Ni–C 1.990(2); C–O 1.312(2); P1–Ni–P2 111.1(1); P2–Ni–C 104.6(1); P1–Ni–O 103.2(1).

Upon treatment of an equimolar solution of **1** and $[\alpha\text{-}^{13}\text{C}]$ -benzaldehyde with stoichiometric H_2SiPh_2 , a new intermediate species forms. This species has a half-life of *ca.* 15 minutes at room temperature. The room temperature $^{13}\text{C}\{^1\text{H}\}$ NMR spectrum of the solution features two singlets at 76.9 ppm and 66.4 ppm, corresponding to the intermediate and the final hydrosilylated product, respectively. In the proton-coupled ^{13}C NMR spectrum, the peak at 76.9 ppm splits into a doublet ($J_{\text{CH}} = 159$ Hz) and the peak at 66.4 ppm splits into a triplet ($J_{\text{CH}} = 142$ Hz). Over the course of the reaction, the resonance associated with the intermediate decays concomitant with growth of the product peak. The intermediate resonance is coupled to a ^1H NMR signal at 5.18 ppm, as determined by 2D HSQC NMR data. In addition, there is a new hydride resonance at -11.4 ppm in the ^1H NMR spectrum. The $^{31}\text{P}\{^1\text{H}\}$ NMR spectrum exhibits a singlet at 38.0 ppm, corresponding to **5** and two doublets centered at 34.9 ($J_{\text{PP}} = 211$ Hz) and 28.0 ppm ($J_{\text{PP}} = 211$ Hz), corresponding to the intermediate species. These three sets of peaks decay over the course of the reaction and at the end of the reaction the only $^{31}\text{P}\{^1\text{H}\}$ NMR resonance is that of **1**. No other $^{31}\text{P}\{^1\text{H}\}$ NMR resonances are observed during the reaction, indicating that $\text{MesDPB}^{\text{Ph}}$ remains bound to Ni throughout. No $^{13}\text{C}\text{-}^{31}\text{P}$ coupling was resolved, even upon cooling to -80°C .

Repeating the reaction under catalytic conditions (5 mol% **1**) yielded spectra with signals analogous to those described above. Fig. 7 shows representative proton-coupled ^{13}C NMR spectra of the catalytic hydrosilylation of $[\alpha\text{-}^{13}\text{C}]$ -benzaldehyde by **1** and H_2SiPh_2 . At -60°C , two resonances are observed immediately after thawing the reaction mixture, corresponding to free aldehyde (192.1 ppm, d, $J_{\text{CH}} = 174$ Hz) and complex **5** (91.3 ppm, d, $J_{\text{CH}} = 174$ Hz) (Fig. 7, top). After 5 min at room temperature and cooling to -60°C , the proton-coupled ^{13}C NMR spectrum features three resonances at 192.1 (d, $J_{\text{CH}} = 174$ Hz), 80.3 (d, $J_{\text{CH}} = 159$ Hz) and 65.6 ppm (t, $J_{\text{CH}} = 142$ Hz), corresponding to

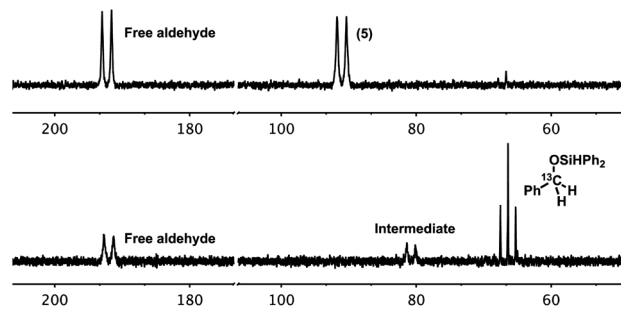


Fig. 7 Representative spectra for catalytic hydrosilylation of $[\alpha\text{-}^{13}\text{C}]$ -benzaldehyde by **1** and H_2SiPh_2 , recorded in toluene- d_8 . (Top) Proton-coupled ^{13}C NMR spectrum recorded at -60°C after thawing the reaction mixture. (Bottom) Proton-coupled ^{13}C NMR spectrum recorded at -60°C after removing from the probe and shaking at room temperature for 5 min.

free aldehyde, the intermediate species and the final hydrosilylated product, respectively (Fig. 7, bottom). Under these conditions, a small amount of a presumably off-path, unidentified Ni complex is also observed by $^{31}\text{P}\{^1\text{H}\}$ NMR spectroscopy. In addition to the peaks corresponding to **5** and the intermediate species, there is another set of doublets centered at 12.7 ($^2J_{\text{PP}} = 294.8$ Hz) and 8.3 ppm ($^2J_{\text{PP}} = 294.8$ Hz); this species does not decay over the course of the reaction and accounts for 6% of the total phosphorus content in solution, as determined by integration at the end of the reaction.

In evaluating the mechanisms and intermediates outlined in Scheme 2, the following considerations are of particular importance:

(1) A hydride resonance is observed in the ^1H NMR spectrum, ruling out [A] as the intermediate species.

(2) In the proton-coupled ^{13}C NMR spectrum, the peak corresponding to the intermediate species splits into a doublet, indicating that only one proton is directly attached to the ^{13}C -labeled carbon atom, thereby ruling out both [A] and [C] as the intermediate species.

(3) Siloxyalkyl complexes of various transition metals have been reported in the literature²⁴ and the ^{13}C NMR shifts of the metal-bound carbon atoms range from 69 ppm to 76 ppm; the ^{13}C NMR shift of the intermediate species for this system (76.9 ppm) is just slightly downfield of this range.

We therefore believe the data to be most consistent with a borohydrido-Ni-siloxyalkyl intermediate species (cycle B, Scheme 2), as in an Ojima-type mechanism. While the aldehyde binds **1** to generate the observable adduct species **5**, this species is off path and productive catalysis can proceed through the borohydrido-Ni-silyl complex **4** via the intermediate [B] in cycle B. We nevertheless caution that our ability to observe intermediate [B] does not preclude the kinetic competence of the other mechanistic cycles shown.

Conclusions

The nickel complex **1** undergoes facile Si–H bond activation to generate new borohydrido-Ni-silyl species. These complexes

have been studied by multinuclear NMR and single crystal X-ray diffraction. The equilibrium process of **4** was studied by ^1H – ^1H 2D EXSY spectroscopy and its kinetic and thermal parameters established. Complex **1** was found to be a competent catalyst for the hydrosilylation of *para*-substituted benzaldehydes and the reaction was determined to be zero order in both aldehyde and silane and first order in catalyst. Stoichiometric reactions with $[\alpha\text{-}^{13}\text{C}]$ -benzaldehyde were undertaken to probe the identity of a reaction intermediate and to reveal a possible catalytic reaction mechanism; based on multinuclear 1D and 2D NMR experiments, a scenario invoking a borohydrido-Ni-siloxyalkyl species is proposed. Further studies will map the scope of these and other E–H bond cleavage processes and probe their application toward organometallic two-electron chemistries better known for noble metal catalysts.

Experimental section

General methods

Unless otherwise noted, all manipulations were carried out using standard Schlenk or glovebox techniques under a dinitrogen atmosphere. Solvents were dried and deoxygenated by sparging with dinitrogen and passing through activated alumina in a solvent purification system from SG Waters USA, LLC. Non-halogenated solvents were tested with a standard purple solution of sodium benzophenone ketyl in tetrahydrofuran in order to confirm effective oxygen and moisture removal. All reagents were purchased from commercial suppliers and used without further purification unless otherwise noted. $[\text{Mes}^*\text{DPB}^{\text{Ph}}]\text{Ni}$ (**1**) and $[\alpha\text{-}^{13}\text{C}]$ -benzaldehyde were synthesized by previously reported procedures.^{9,25} D_2SiPh_2 was prepared via LAD reduction of Cl_2SiPh_2 in OEt_2 . Elemental analyses were performed by Midwest Microlab, LLC, Indianapolis, IN and Robertson Microlit Laboratories, Inc., Ledge-wood, NJ. Deuterated solvents were purchased from Cambridge Isotope Laboratories, Inc., degassed, and dried over activated 3 Å molecular sieves prior to use. ^1H and ^{13}C chemical shifts are reported in ppm relative to SiMe_4 using residual solvent ^1H and ^{13}C resonances as internal standards. ^{31}P , ^{11}B and ^{29}Si chemical shifts are reported in ppm relative to 85% aqueous H_3PO_4 , $\text{BF}_3 \cdot \text{Et}_2\text{O}$ and SiMe_4 , respectively. GC-MS analyses were performed on an Agilent Technologies 6890N GC system with an HP-5MS column.

Preparation of $[\text{Mes}^*\text{DPB}^{\text{Ph}}](\mu\text{-H})\text{NiSiH}_2\text{Ph}$ (**3**)

To a solution of **1** (44.5 mg, 62.6 μmol) in benzene (1 mL) was added neat H_3SiPh (7.8 μL , 63.2 μmol). The solution was stirred 2 h at room temperature and pentane was added to precipitate an orange powder. The slurry was stirred for another 30 min and the solids collected on a glass-sintered frit. The solids were washed with pentane and dried *in vacuo* (36.6 mg, 71%). Crystals suitable for X-ray analysis were grown from a concentrated ether solution. ^1H NMR (400 MHz, C_6D_6) δ 7.63 (q, $J = 5.8$ Hz, 4H), 7.52 (d, $J = 7.4$ Hz, 2H), 7.33–7.22 (m, 6H), 7.14–7.07 (m, 4H), 7.06–6.82 (m, 17H), 6.43 (s, 2H), 4.30 (t, $^3J_{\text{HP}} = 9.2$ Hz, $^1J_{\text{HSi}} = 138$ Hz, 2H), 2.14 (s, 3H), 1.93 (s, 6H), -2.47 (s, 1H). ^{13}C

$\{^1\text{H}\}$ NMR (101 MHz, C_6D_6) δ 141.2, 136.5, 135.0, 133.8, 133.5, 130.6, 130.0, 129.8, 129.6, 128.9, 127.0, 126.3, 25.2, 20.6. $^{31}\text{P}\{^1\text{H}\}$ NMR (162 MHz, C_6D_6) δ 41.1 (s). $^{29}\text{Si}\{^1\text{H}\}$ (79 MHz, C_6D_6) δ -17.0 (t, $J = 38.7$ Hz). $^{11}\text{B}\{^1\text{H}\}$ (128 MHz, C_6D_6) δ -2.2. IR (KBr, cm^{-1}): 2060. Anal. calcd for $\text{C}_{51}\text{H}_{47}\text{BNiP}_2\text{Si}\cdot\text{OEt}_2$: C, 73.93; H, 6.41. Found: C, 74.05; H, 6.13.

Preparation of $[\text{Mes}^{\text{DPB}}\text{Ph}](\mu\text{-H})\text{NiSiHPh}_2$ (4)

To a solution of **1** (59.4 mg, 83.5 μmol) in benzene (1 mL) was added neat H_2SiPh_2 (16.4 μL , 88.1 μmol). The solution was stirred 2 h at room temperature and pentane was added to precipitate a yellow powder. The slurry was stirred for another 30 min and the solids collected on a glass-sintered frit. The solids were washed with pentane and dried *in vacuo* (56.8 mg, 76%). ^1H NMR (400 MHz, *tol-d*₈) δ 7.69 (s, 4H), 7.43 (d, $J = 7.5$ Hz, 2H), 7.18 (s, 2H), 7.15–6.91 (m, 20H), 6.89–6.76 (m, 6H), 6.71–6.60 (m, 4H), 6.33 (s, 2H), 5.01 (t, $^3J_{\text{HP}} = 14.7$ Hz, $^1J_{\text{HSi}} = 88$ Hz, 1H), 2.11 (s, 3H), 1.84 (s, 6H), -2.61 (s, 1H). $^{13}\text{C}\{^1\text{H}\}$ NMR (101 MHz, C_6D_6) δ 141.2, 139.3, 137.1, 136.3, 135.6, 134.1, 133.8, 133.1, 130.5, 129.9, 129.8, 129.3, 128.9, 127.5, 127.4, 127.0, 126.3, 124.5, 25.4, 20.6. $^{31}\text{P}\{^1\text{H}\}$ NMR (162 MHz, C_6D_6) δ 40.9 (s). $^{29}\text{Si}\{^1\text{H}\}$ (79 MHz, C_6D_6) δ 3.1 (t, $J = 37.9$ Hz). $^{11}\text{B}\{^1\text{H}\}$ (128 MHz, C_6D_6) δ -1.7. IR (KBr, cm^{-1}): 2058. Anal. calcd for $\text{C}_{57}\text{H}_{51}\text{BNiP}_2\text{Si}$: C, 76.45; H, 5.78. Found: C, 76.03; H, 5.99.

Preparation of $[\text{Mes}^{\text{DPB}}\text{Ph}]\text{Ni}(\eta^2\text{-benzaldehyde})$ (5)

To a slurry of **1** (53.2 mg, 74.8 μmol) in pentane (15 mL) was added neat benzaldehyde (7.7 μL , 75.5 μmol). The slurry was stirred 2 h at room temperature, during which time brown-red microcrystalline material precipitated. The solids were collected on a glass-sintered frit and washed with pentane, then dried *in vacuo* (48.2 mg, 78%). ^1H NMR (500 MHz, C_6D_6) δ 7.77–7.59 (m, 4H), 7.07–6.87 (m, 14H), 6.87–6.71 (m, 7H), 6.68 (d, $J = 4.7$ Hz, 4H), 6.50 (s, 2H), 6.48–6.38 (m, 4H), 6.25 (s, 1H), 2.35 (s, 6H), 2.07 (s, 3H). $^{13}\text{C}\{^1\text{H}\}$ NMR (126 MHz, C_6D_6) δ 161.9, 145.7, 144.0, 140.0, 134.2, 132.5, 132.3, 139.6, 128.7, 126.5, 125.2, 124.7, 84.1, 26.9, 21.0. $^{31}\text{P}\{^1\text{H}\}$ NMR (202 MHz, C_6D_6) δ 38.6 (s). $^{11}\text{B}\{^1\text{H}\}$ (128 MHz, C_6D_6) δ 58.2 (br). Anal. calcd for $\text{C}_{52}\text{H}_{45}\text{BNiOP}_2$: C, 76.41; H, 5.55. Found: C, 76.03; H, 5.99.

Hydrosilylation studies

In a typical experiment, a J. Young NMR tube was charged with **1** (100 μL , 0.039 M in C_6D_6), substrate (20 eq. relative to **1**), ferrocene (83 μL , 0.236 M in C_6D_6), C_6D_6 and frozen. Once frozen, H_2SiPh_2 (20 eq. relative to **1**) was added and the tube frozen (total volume = 600 μL). Once at the spectrometer, the solution was thawed and spectra collected at regular intervals. After completion, the reaction mixture was then exposed to air, diluted with toluene, filtered through a plug of silica and analyzed by GC-MS. Hydrosilylation products were identified using ^1H NMR and GC-MS data in comparison to the literature data.^{13,26} To aid characterization, (1-(4-trifluoromethylphenyl)-methoxy)diphenylsilane was converted to 4-(trifluoromethyl)-phenyl methanol by treatment with 1 M HCl; the ^1H NMR and GC-MS data obtained agree with the literature data.²⁷

Mercury tests for homogeneity

Method 1. A solution of **1** (30 μL , 0.061 M, 5 mol%) in C_6D_6 was stirred with excess Hg (72.6 mg, *ca.* 200 eq. per Ni atom) for 15 min. A solution of *p*-dimethylaminobenzaldehyde (5.2 mg, 34.8 μmol) and H_2SiPh_2 (6.5 μL , 35.0 μmol) in C_6D_6 was added and the mixture stirred at 23 °C for 2 h. The solution was then filtered through Celite and analyzed by ^1H NMR spectroscopy. Complete hydrosilylation was observed in the time expected.

Method 2. **1** (30 μL , 0.061 M, 5 mol%) was added to a C_6D_6 solution of *p*-dimethylaminobenzaldehyde (5.2 mg, 34.8 μmol) and H_2SiPh_2 (6.5 μL , 35.0 μmol). The resulting solution was stirred for 5 min at 23 °C, then added to Hg (46.5 mg, *ca.* 125 eq. per Ni atom) and stirred for 2 h at 23 °C. The solution was then filtered through Celite and analyzed by ^1H NMR spectroscopy. Complete hydrosilylation was observed in the time expected.

Variable temperature solution NMR studies

Equilibrium of 1 and 4. Ferrocene and **4** were dissolved in toluene-*d*₈ and transferred to a J. Young NMR tube. The tube was inserted into a temperature controlled NMR probe and ^1H NMR spectra were collected at 10 K intervals from 328 K to 368 K, allowing 20 min for equilibration at each temperature. The concentration of **1** and **4** were determined by integration of the mesityl aryl C–H resonance for the respective complexes and silane concentration was assumed to be equal to that of **1**. Details concerning the calculation of the thermal parameters are given in the ESI.†

Equilibrium of 1 and $[\text{Mes}^{\text{DPB}}\text{Ph}](\text{D})\text{NiSiDPh}_2$ (4-D). Ferrocene and an equimolar amount of D_2SiPh_2 and **1** were dissolved in toluene-*d*₈ and transferred to a J. Young NMR tube. The tube was inserted into a temperature controlled NMR probe and ^1H NMR spectra were collected at 10 K intervals from 298 K to 358 K, allowing 20 min for equilibration at each temperature. Concentrations of **1** and **4-D** were determined by integration of the mesityl aryl C–H resonance for the respective complexes and silane concentration was assumed to be equal to that of **1**. Details concerning the calculation of the thermal parameters are given in the ESI.†

^1H - ^1H EXSY study of the equilibrium of 1 and 4. 2D ^1H - ^1H EXSY spectra were collected using the samples prepared for the variable temperature experiments outline above. To determine the exchange rates of the equilibrium between **1** and **4**, two 2D EXSY experiments were acquired (mixing times (T_m) of 0 ms and 700 ms) at 10 K intervals from 328 K to 358 K, allowing 30 min for equilibration at each temperature. Details and a discussion concerning the extraction of the kinetic parameters are given in the ESI.†

Crystallographic information

Low-temperature single crystal X-ray diffraction studies were carried out at the Beckman Institute Crystallography Facility on a Bruker Kappa Apex II diffractometer with Mo $K\alpha$ radiation ($\lambda = 0.71073$ Å). Structures were solved by direct or Patterson methods using SHELXS²⁸ and refined against F^2 on all data by

full-matrix least squares with SHELXL-97 (ref. 29) using established techniques.³⁰ Full details are given in the ESI.†

Acknowledgements

This work was supported by the National Science Foundation Center for Chemical Innovation on Solar Fuels (CCI Solar, Grant CHE-1305124) and the Gordon and Betty Moore Foundation. We thank David VanderVelde for assistance with NMR experiments.

Notes and references

- (a) A. M. Tondreau, C. C. H. Atienza, K. J. Weller, S. A. Nye, K. M. Lewis, J. G. P. Delis and P. J. Chirik, *Science*, 2012, **335**, 567; (b) J. Y. Corey, *Chem. Rev.*, 2011, **111**, 863; (c) B. Marciniak, H. Maciejewski, C. Pietraszuk and P. Pawluc, in *Hydrosilylation: A Comprehensive Review on Recent Advances*, ed. B. Marciniak, Springer, Berlin, 2009; (d) I. E. Markó, S. Stérin, O. Buisine, G. Mignani, P. Branlard, B. Tinant and J. Declercq, *Science*, 2002, **298**, 204.
- J. Tang and T. Hayashi, in *Catalytic Heterofunctionalization*, ed. A. Togni and H. Grützmacher, Wiley-VCH Verlag GmbH, Weinheim, Germany, 2001.
- (a) S. Shimada and M. Tanaka, *Coord. Chem. Rev.*, 2006, **250**, 991; (b) J. Y. Corey and J. Braddock-Wilking, *Chem. Rev.*, 1999, **99**, 175.
- (a) N. Nakata, S. Fukazawa, N. Kato and A. Ishii, *Organometallics*, 2011, **30**, 4490; (b) R. C. Boyle, J. T. Mague and M. J. Fink, *J. Am. Chem. Soc.*, 2003, **125**, 3228.
- (a) J. Braddock-Wilking, Y. Zhang, J. Y. Corey and N. P. Rath, *J. Organomet. Chem.*, 2008, **693**, 1233; (b) H. Arii, M. Takahashi, A. Noda, M. Nanjo and K. Mochida, *Organometallics*, 2008, **27**, 1929; (c) D. Chan, S. B. Duckett, S. L. Heath, I. G. Khazal, R. N. Perutz, S. Sabo-Etienne and P. L. Timmins, *Organometallics*, 2004, **23**, 5744; (d) R. S. Simons, L. M. Sanow, K. J. Galat, C. A. Tessier and W. J. Youngs, *Organometallics*, 2000, **19**, 3994; (e) H. Azizian, K. R. Dixon, C. Eaborn, A. Pidcock, N. M. Shuaib and J. Vinaixa, *J. Chem. Soc., Chem. Commun.*, 1982, 1020; (f) C. Eaborn, A. Pidcock and B. Ratcliff, *J. Organomet. Chem.*, 1972, **43**, C5.
- (a) V. M. Iluc and G. L. Hillhouse, *J. Am. Chem. Soc.*, 2010, **132**, 11890; (b) E. E. Smith, G. Du, P. E. Fanwick and M. M. Abu-Omar, *Organometallics*, 2010, **29**, 6527; (c) D. Adhikari, M. Pink and D. J. Mindiola, *Organometallics*, 2009, **28**, 2072; (d) M. T. Whited, N. P. Mankad, Y. Lee, P. F. Oblad and J. C. Peters, *Inorg. Chem.*, 2009, **48**, 2507; (e) S. O. Kang, J. Lee and J. Ko, *Coord. Chem. Rev.*, 2002, **231**, 47.
- (a) J. Takaya and N. Iwasawa, *Dalton Trans.*, 2011, **40**, 8814; (b) V. M. Iluc and G. L. Hillhouse, *Tetrahedron*, 2006, **62**, 7577; (c) W. Chen, S. Shimada, M. Tanaka, Y. Kobayashi and K. Saigo, *J. Am. Chem. Soc.*, 2004, **126**, 8072.
- (a) C. Tsay and J. C. Peters, *Chem. Sci.*, 2012, **3**, 1313; (b) T. Zell, T. Schaub, K. Radacki and U. Radius, *Dalton Trans.*, 2011, **40**, 1852.
- W. H. Harman and J. C. Peters, *J. Am. Chem. Soc.*, 2012, **134**, 5080.
- (a) F. Hoffmann, U. Böhme and G. Roewer, *Z. Naturforsch., B: J. Chem. Sci.*, 2009, **64**, 1423; (b) T. Schaub, C. Döring and U. Radius, *Dalton Trans.*, 2007, 1993; (c) T. Steinke, C. Gemel, M. Cokoja, M. Winter and R. A. Fischer, *Angew. Chem., Int. Ed.*, 2004, **43**, 2299; (d) S. Nlate, E. Herdtweck and R. A. Fischer, *Angew. Chem., Int. Ed.*, 1996, **35**, 1861; (e) M. M. Brezinski, J. Schneider, L. J. Radonovich and K. J. Klabunde, *Inorg. Chem.*, 1989, **28**, 2414; (f) T. R. Bierschenk, M. A. Guerra, T. J. Juhlke, S. B. Larson and R. J. Lagow, *J. Am. Chem. Soc.*, 1987, **109**, 4855.
- D. G. Churchill, K. E. Janak, J. S. Wittenberg and G. Parkin, *J. Am. Chem. Soc.*, 2003, **125**, 1403.
- (a) A. Pastor and E. Martínez-Viviente, *Coord. Chem. Rev.*, 2008, **252**, 2314; (b) M. Pons and O. Millet, *Prog. Nucl. Magn. Reson. Spectrosc.*, 2001, **38**, 267.
- A. M. Tondreau, E. Lobkovsky and P. J. Chirik, *Org. Lett.*, 2008, **10**, 2789.
- (a) H. Nishiyama, in *Comprehensive Chirality*, ed. E. M. Carreira and H. Yamamoto, Elsevier, Amsterdam, 2012; (b) K. Riener, M. P. Högerl, P. Gigler and F. E. Kühn, *ACS Catal.*, 2012, **2**, 613; (c) K. Yamamoto and T. Hayashi, in *Transition Metals for Organic Synthesis*, ed. M. Beller and C. Bolm, Wiley-VCH Verlag GmbH, Weinheim, Germany, 2008.
- (a) D. J. Ramón and M. Yus, *Chem. Rev.*, 2006, **106**, 2126; (b) M. Bandini, F. Bernardi, A. Bottoni, P. G. Cozzi, G. P. Miscione and A. Umani-Ronchi, *Eur. J. Org. Chem.*, 2003, **15**, 2972; (c) P. Beagley, P. J. Davies, A. J. Blacker and C. White, *Organometallics*, 2002, **21**, 5852; (d) J. Yun and S. L. Buchwald, *J. Am. Chem. Soc.*, 1999, **121**, 5640.
- (a) M. Darwish and M. Wills, *Catal. Sci. Technol.*, 2012, **2**, 243; (b) K. Junge, K. Schröder and M. Beller, *Chem. Commun.*, 2011, **47**, 4849; (c) P. J. Chirik, in *Catalysis without Precious Metals*, ed. R. M. Bullock, Wiley-VCH Verlag GmbH & Co. KGaA, Weinheim, Germany, 2010; (d) J. Yang and T. D. Tilley, *Angew. Chem., Int. Ed.*, 2010, **49**, 10186; (e) M. Zhang and A. Zhang, *Appl. Organomet. Chem.*, 2010, **24**, 751; (f) R. H. Morris, *Chem. Soc. Rev.*, 2009, **38**, 2282.
- (a) S. Kundu, W. W. Brennessel and W. D. Jones, *Inorg. Chem.*, 2011, **50**, 9443; (b) B. L. Tran, M. Pink and D. J. Mindiola, *Organometallics*, 2009, **28**, 2234; (c) S. Chakraborty, J. A. Krause and H. Guan, *Organometallics*, 2009, **28**, 582; (d) F.-G. Fontaine and D. Zargarian, *Organometallics*, 2002, **21**, 401.
- (a) B. H. Lipshutz, *Synlett*, 2009, **4**, 509; (b) S. Díez-González and S. P. Nolan, *Acc. Chem. Res.*, 2008, **41**, 349; (c) S. Rendler and M. Oestreich, *Angew. Chem., Int. Ed.*, 2007, **46**, 498.
- I. Ojima, T. Kogure, M. Kumagai, S. Horiuchi and T. Sato, *J. Organomet. Chem.*, 1976, **122**, 83.
- G. Z. Zheng and T. H. Chan, *Organometallics*, 1995, **14**, 70.
- C. A. Tolman, A. D. English and L. E. Manzer, *Inorg. Chem.*, 1975, **14**, 2353.
- (a) I. Matas, J. Cámpora, P. Palma and E. Álvarez, *Organometallics*, 2009, **28**, 6515; (b) S. Ogoshi, M. Ueta,

- T. Arai and H. Kurosawa, *J. Am. Chem. Soc.*, 2005, **127**, 12810; (c) D. Walther, *J. Organomet. Chem.*, 1980, **190**, 393.
- 23 (a) D. J. Mindiola, R. Waterman, D. M. Jenkins and G. L. Hillhouse, *Inorg. Chim. Acta*, 2003, **345**, 299; (b) J. Kaiser, J. Sieler, D. Walther, E. Dinjus and L. Golic, *Acta Crystallogr., Sect. B: Struct. Crystallogr. Cryst. Chem.*, 1982, **38**, 1584; (c) T. T. Tsou, J. C. Huffman and J. K. Kochi, *Inorg. Chem.*, 1979, **18**, 2311; (d) R. Countryman and B. R. Penfold, *J. Cryst. Mol. Struct.*, 1972, **2**, 281; (e) R. Countryman and B. R. Penfold, *J. Chem. Soc., Chem. Commun.*, 1971, **24**, 1598.
- 24 (a) M. Akita, O. Mitani, M. Sayama and Y. Moro-oka, *Organometallics*, 1991, **10**, 1394; (b) B. T. Gregg, P. K. Hanna, E. J. Crawford and A. R. Cutler, *J. Am. Chem. Soc.*, 1991, **113**, 384; (c) P. K. Hanna, B. T. Gregg and A. R. Cutler, *Organometallics*, 1991, **10**, 31; (d) M. Akita, O. Mitani and Y. Moro-oka, *J. Chem. Soc., Chem. Commun.*, 1989, 527; (e) J. C. Selover, G. D. Vaughn, C. E. Strouse and J. A. Gladysz, *J. Am. Chem. Soc.*, 1986, **108**, 1455; (f) J. A. Gladysz, *Acc. Chem. Res.*, 1984, **17**, 326.
- 25 M. E. Blake, K. L. Bartlett and M. Jones Jr, *J. Am. Chem. Soc.*, 2003, **125**, 6485.
- 26 Y. Wei, S. Han, J. Kim, S. Soh and B. A. Grzybowski, *J. Am. Chem. Soc.*, 2010, **132**, 11018.
- 27 G. Nagendra, C. Madhu, T. M. Vishwanatha and V. V. Sureshbabu, *Tetrahedron Lett.*, 2012, **53**, 5059.
- 28 G. M. Sheldrick, *Acta Crystallogr., Sect. A: Found. Crystallogr.*, 1990, **46**, 467.
- 29 G. M. Sheldrick, *Acta Crystallogr., Sect. A: Found. Crystallogr.*, 2008, **64**, 112.
- 30 P. Müller, *Crystallogr. Rev.*, 2009, **15**, 57.